

UCLA

UCLA Previously Published Works

Title

Advances in Photoplethysmography for Personalized Cardiovascular Monitoring

Permalink

<https://escholarship.org/uc/item/4fn998sz>

Journal

Biosensors, 12(10)

ISSN

2079-6374

Authors

Kim, Seamin
Xiao, Xiao
Chen, Jun

Publication Date

2022



DOI

10.3390/bios12100863

Peer reviewed

Editorial

Advances in Photoplethysmography for Personalized Cardiovascular Monitoring

Seamin Kim ¹, Xiao Xiao ²  and Jun Chen ^{2,*} ¹ Department of Physics and Astronomy, University of California, Irvine, CA 92697, USA² Department of Bioengineering, University of California, Los Angeles, CA 90095, USA

* Correspondence: jun.chen@ucla.edu

Abstract: Photoplethysmography (PPG) is garnering substantial interest due to low cost, noninvasiveness, and its potential for diagnosing cardiovascular diseases, such as cardiomyopathy, heart failure, and arrhythmia. The signals obtained through PPG can yield information based on simple analyses, such as heart rate. In contrast, when accompanied by the complex analysis of sophisticated signals, valuable information, such as blood pressure, sympathetic nervous system activity, and heart rate variability, can be obtained. For a complex analysis, a better understanding of the sources of noise, which create limitations in the application of PPG, is needed to get reliable information to assess cardiovascular health. Therefore, this Special Issue handles literature about noises and how they affect the waveform of the PPG caused by individual variations (e.g., skin tone, obesity, age, and gender), physiology (e.g., respiration, venous pulsation, body site of measurement, and body temperature), and external factors (e.g., motion artifact, ambient light, and applied pressure to the skin). It also covers the issues that still need to be considered in each situation.

Keywords: photoplethysmography; cardiovascular disease; biosignal monitoring



Citation: Kim, S.; Xiao, X.; Chen, J. Advances in Photoplethysmography for Personalized Cardiovascular Monitoring. *Biosensors* **2022**, *12*, 863. <https://doi.org/10.3390/bios12100863>

Received: 28 September 2022

Accepted: 10 October 2022

Published: 12 October 2022

Publisher's Note: MDPI stays neutral with regard to jurisdictional claims in published maps and institutional affiliations.



Copyright: © 2022 by the authors. Licensee MDPI, Basel, Switzerland. This article is an open access article distributed under the terms and conditions of the Creative Commons Attribution (CC BY) license (<https://creativecommons.org/licenses/by/4.0/>).

The continuous/intermittent monitoring system based on biosignals can deliver preventive treatment because it can measure abnormal body signals and obtain information such as disease therapy effects [1–8]. Photoplethysmography (PPG), which gets the biosignals related to blood flow with light-emitting diodes and photodetector, is one of the promising monitoring systems, since it enables the diagnosis of diseases directly related to human lives, such as information related to cardiovascular disease (CVD) [9–13]. CVD is a class of chronic conditions and the number one cause of death globally, contributing to more than 17 million deaths [14–16]. PPG is one of the noninvasive methods for diagnosing and monitoring these cardiovascular diseases. As it is a noninvasive method, an accurate analysis of the signal obtained from the photodetector is required.

The photodetector collects the transmitted or reflected light depending on the contraction and relaxation of the artery, and we can get the changes in blood flow by analyzing the electrical signals [17]. The periodically changing signals obtain pulsatile information, and changes in light transmittance show changes in erythrocyte orientation [18]. The PPG waveform, a periodic AC pulsatile component of electrical signals by removing the quasi-DC baseline component, has tremendous information to assess cardiovascular health. We can get (i) heart rate, stroke volume, and hypertension by PPG waveform, (ii) blood velocity by the first derivative, and (iii) vascular health and risk for cardiovascular disease by the second derivative [19–25]. Despite the usefulness of these PPGs, the devices approved by U.S. Food and Drug Administration are limited because of the numerous sources of noise that can impede the output of the PPG [26]. For true health monitoring, these sources of noise and how they affect the waveform of the PPG and its derivatives should be resolved.

The PPG exhibits varied responses in the following conditions: (i) individual variations, (ii) physiological processes, and (iii) external environments. First, we will discuss the factors in the individual variations (e.g., skin tone, obesity, age, and gender) that affect

the PPG characteristics. Although the PPG-emitted green light (wavelength: ~550 nm) is relatively insensitive to the melamine content, the PPG signals exhibit a low signal-to-noise ratio in a darker skin tone [27,28]. Obesity is also a primary factor for the PPG system because it can induce multiple changes in the subject's metabolism (e.g., skin thickness, blood flow, capillary density, etc.) [29,30]. Furthermore, aging that influences the cardiovascular system, skin thickness, and degree of hydration may dampen the PPG resolution [31]. The waveform of the PPG signals can differ in response to the gender-associated physiological differences that involve blood pressure, heart mass, and average heart rate [32]. Therefore, to achieve a high signal-to-noise ratio (SNR), a more optimized PPG system should be established through data library and machine learning [33–38].

Next, physiological processes (e.g., respiration, venous pulsations, local body temperature, etc.) mainly affect the PPG waveform. For example, variations in respiratory characteristics produce significant changes in the PPG signals with different intensities, amplitude, and frequencies [39–41]. Likewise, venous pulsation yields periodical AC signals resulting from the blood volume changes, which is detrimental to accurate PPG measurement [42,43]. Local body temperature is also found to be positively proportional to the amplitude of the PPG signals [44,45]. Therefore, for precise analysis of the PPG signals, the baseline signals from the physiological processes need to be observed for the post-signal processing.

At last, external factors may modify the noise level of the PPG signals. For example, biomechanical motions with varied frequency ranges induce the fluctuation of the PPG signals [46]. Besides, previous studies state that ambient light limits the accuracy of the PPG measurements with the increased noise level [47]. Thus, these potential external factors need to be controlled and consistent to achieve a more reliable PPG measurement.

In this editorial we have discussed significant challenges to securing the accuracy of the PPG measurements according to the accepted topic. We look forward to advancing the PPG measurements resulting in a precise, personalized technique for the biosignal monitoring system. Moreover, benefiting from its low-power consumption feature, we suggest that energy harvesting technologies and flexible energy storage can be a promising solution for the energy source of PPG-integrated medical devices [48–54]. Thus, we expect the wearable PPG-based diagnostic system to provide an exceptional clinical experience to patients.

Funding: J.C. acknowledges the Hellman Fellows Research Grant and the BBRF Young Investigator Grant.

Acknowledgments: J.C. acknowledge the Henry Samueli School of Engineering & Applied Science and the Department of Bioengineering at the University of California, Los Angeles for the startup support, and the UCLA Pandemic Resources Program Research Award, and the Research Recovery Grant by the UCLA Academic Senate.

Conflicts of Interest: The authors declare no conflict of interest.

References

1. Meng, K.; Zhao, S.; Zhou, Y.; Wu, Y.; Zhang, S.; He, Q.; Wang, X.; Zhou, Z.; Fan, W.; Tan, X.; et al. A Wireless Textile-Based Sensor System for Self-Powered Personalized Health Care. *Matter* **2020**, *2*, 896–907. [[CrossRef](#)]
2. Xiao, X.; Yin, J.; Chen, G.; Shen, S.; Nashalian, A.; Chen, J. Bioinspired Acoustic Textiles with Nanoscale Vibrations for Wearable Biomonitoring. *Matter* **2022**, *5*, 1342–1345. [[CrossRef](#)]
3. Chen, G.; Xiao, X.; Zhao, X.; Tat, T.; Bick, M.; Chen, J. Electronic Textiles for Wearable Point-of-Care Systems. *Chem Rev* **2022**, *122*, 3259–3291. [[CrossRef](#)] [[PubMed](#)]
4. Zhang, S.; Bick, M.; Xiao, X.; Chen, G.; Nashalian, A.; Chen, J. Leveraging Triboelectric Nanogenerators for Bioengineering. *Matter* **2021**, *4*, 845–887. [[CrossRef](#)]
5. Zhao, X.; Zhou, Y.; Xu, J.; Chen, G.; Fang, Y.; Tat, T.; Xiao, X.; Song, Y.; Li, S.; Chen, J. Soft Fibers with Magnetoelasticity for Wearable Electronics. *Nat. Commun.* **2021**, *12*, 6755. [[CrossRef](#)] [[PubMed](#)]
6. Libanori, A.; Chen, G.; Zhao, X.; Zhou, Y.; Chen, J. Smart Textiles for Personalized Healthcare. *Nat. Electron.* **2022**, *5*, 142–156. [[CrossRef](#)]
7. Xiao, X.; Chen, G.; Libanori, A.; Chen, J. Wearable Triboelectric Nanogenerators for Therapeutics. *Trends Chem.* **2021**, *3*, 279–290. [[CrossRef](#)]

8. Zhou, Z.; Chen, K.; Li, X.; Zhang, S.; Wu, Y.; Zhou, Y.; Meng, K.; Sun, C.; He, Q.; Fan, W.; et al. Sign-to-Speech Translation Using Machine-Learning-Assisted Stretchable Sensor Arrays. *Nat. Electron.* **2020**, *3*, 571–578. [[CrossRef](#)]
9. Elgendi, M.; Fletcher, R.; Liang, Y.; Howard, N.; Lovell, N.H.; Abbott, D.; Lim, K.; Ward, R. The Use of Photoplethysmography for Assessing Hypertension. *Npj Digit. Med.* **2019**, *2*, 60. [[CrossRef](#)] [[PubMed](#)]
10. Meng, K.; Xiao, X.; Liu, Z.; Shen, S.; Tat, T.; Wang, Z.; Lu, C.; Ding, W.; He, X.; Yang, J.; et al. Kirigami-Inspired Pressure Sensors for Wearable Dynamic Cardiovascular Monitoring. *Adv. Mater.* **2022**, *34*, 2202478. [[CrossRef](#)]
11. Kireev, D.; Sel, K.; Ibrahim, B.; Kumar, N.; Akbari, A.; Jafari, R.; Akinwande, D. Continuous Cuffless Monitoring of Arterial Blood Pressure via Graphene Bioimpedance Tattoos. *Nat. Nanotechnol.* **2022**, 1–7. [[CrossRef](#)]
12. Meng, K.; Chen, J.; Li, X.; Wu, Y.; Fan, W.; Zhou, Z.; He, Q.; Wang, X.; Fan, X.; Zhang, Y.; et al. Flexible Weaving Constructed Self-Powered Pressure Sensor Enabling Continuous Diagnosis of Cardiovascular Disease and Measurement of Cuffless Blood Pressure. *Adv. Funct. Mater.* **2019**, *29*, 1806388. [[CrossRef](#)]
13. Chen, G.; Au, C.; Chen, J. Textile Triboelectric Nanogenerators for Wearable Pulse Wave Monitoring. *Trends Biotechnol.* **2021**, *39*, 1078–1092. [[CrossRef](#)] [[PubMed](#)]
14. Meng, K.; Xiao, X.; Wei, W.; Chen, G.; Nashalian, A.; Shen, S.; Xiao, X.; Chen, J. Wearable Pressure Sensors for Pulse Wave Monitoring. *Adv. Mater.* **2022**, *34*, 2109357. [[CrossRef](#)]
15. Shen, S.; Xiao, X.; Xiao, X.; Chen, J. Wearable Triboelectric Nanogenerators for Heart Rate Monitoring. *Chem. Commun.* **2021**, *57*, 5871–5879. [[CrossRef](#)] [[PubMed](#)]
16. Fang, Y.; Zou, Y.; Xu, J.; Chen, G.; Zhou, Y.; Deng, W.; Zhao, X.; Roustaei, M.; Hsiai, T.K.; Chen, J. Ambulatory Cardiovascular Monitoring Via a Machine-Learning-Assisted Textile Triboelectric Sensor. *Adv. Mater.* **2021**, *33*, 2104178. [[CrossRef](#)] [[PubMed](#)]
17. Deng, W.; Zhou, Y.; Tat, T.; Xu, S.; Jin, H.; Li, W.; Chun, F.; Yan, C.; Yang, W.; Chen, J. A Perovskite-Based Photodetector with Enhanced Light Absorption, Heat Dissipation, and Humidity Stability. *Adv. Photonics Res.* **2021**, *2*, 2100123. [[CrossRef](#)]
18. Lindberg, L.-G.; Oberg, P.A. Optical Properties of Blood in Motion. *Opt Eng.* **1993**, *32*, 253–257. [[CrossRef](#)]
19. Castaneda, D.; Esparza, A.; Ghamari, M.; Soltanpur, C.; Nazeran, H. A Review on Wearable Photoplethysmography Sensors and Their Potential Future Applications in Health Care. *Int. J. Biosens. Bioelectron.* **2018**, *4*, 195–202. [[CrossRef](#)]
20. Fujita, D.; Suzuki, A. Evaluation of the Possible Use of PPG Waveform Features Measured at Low Sampling Rate. *IEEE Access* **2019**, *7*, 58361–58367. [[CrossRef](#)]
21. Rajala, S.; Lindholm, H.; Taipalus, T. Comparison of Photoplethysmogram Measured from Wrist and Finger and the Effect of Measurement Location on Pulse Arrival Time. *Physiol. Meas.* **2018**, *39*, 075010. [[CrossRef](#)] [[PubMed](#)]
22. Uçar, M.K.; Bozkurt, M.R.; Bilgin, C.; Polat, K. Automatic Sleep Staging in Obstructive Sleep Apnea Patients Using Photoplethysmography, Heart Rate Variability Signal and Machine Learning Techniques. *Neural Comput. Appl.* **2018**, *29*, 1–16. [[CrossRef](#)]
23. Liang, Y.; Chen, Z.; Ward, R.; Elgendi, M. Hypertension Assessment via ECG and PPG Signals: An Evaluation Using MIMIC Database. *Diagnostics* **2018**, *8*, 65. [[CrossRef](#)]
24. Takazawa, K.; Tanaka, N.; Fujita, M.; Matsuoka, O.; Saiki, T.; Aikawa, M.; Tamura, S.; Ibukiyama, C. Assessment of Vasoactive Agents and Vascular Aging by the Second Derivative of Photoplethysmogram Waveform. *Hypertension* **1998**, *32*, 365–370. [[CrossRef](#)]
25. Elgendi, M.; Liang, Y.; Ward, R. Toward Generating More Diagnostic Features from Photoplethysmogram Waveforms. *Diseases* **2018**, *6*, 20. [[CrossRef](#)] [[PubMed](#)]
26. Fine, J.; Branam, K.L.; Rodriguez, A.J.; Boonya-ananta, T.; Ajmal; Ramella-Roman, J.C.; McShane, M.J.; Coté, G.L. Sources of Inaccuracy in Photoplethysmography for Continuous Cardiovascular Monitoring. *Biosensors* **2021**, *11*, 126. [[CrossRef](#)]
27. Thody, A.J.; Higgins, E.M.; Wakamatsu, K.; Ito, S.; Burchill, S.A.; Marks, J.M. Pheomelanin as Well as Eumelanin Is Present in Human Epidermis. *J. Investig. Dermatol.* **1991**, *97*, 340–344. [[CrossRef](#)]
28. Preejith, S.P.; Alex, A.; Joseph, J.; Sivaprakasam, M. Design, Development and Clinical Validation of a Wrist-Based Optical Heart Rate Monitor. In Proceedings of the 2016 IEEE International Symposium on Medical Measurements and Applications (MeMeA), Benevento, Italy, 15–18 May 2016; pp. 1–6. [[CrossRef](#)]
29. Gibney, M.A.; Arce, C.H.; Byron, K.J.; Hirsch, L.J. Skin and Subcutaneous Adipose Layer Thickness in Adults with Diabetes at Sites Used for Insulin Injections: Implications for Needle Length Recommendations. *Curr. Med. Res. Opin.* **2010**, *26*, 1519–1530. [[CrossRef](#)] [[PubMed](#)]
30. Limberg, J.K.; Morgan, B.J.; Schrage, W.G. Peripheral Blood Flow Regulation in Human Obesity and Metabolic Syndrome. *Exerc. Sport Sci. R.* **2016**, *44*, 116–122. [[CrossRef](#)] [[PubMed](#)]
31. Mulder, T.J.S.V.; de Koeijer, M.; Theeten, H.; Willems, D.; Damme, P.V.; Demolder, M.; Meyer, G.D.; Beyers, K.C.L.; Vankerckhoven, V. High Frequency Ultrasound to Assess Skin Thickness in Healthy Adults. *Vaccine* **2017**, *35*, 1810–1815. [[CrossRef](#)]
32. Dao, H.; Kazin, R.A. Gender Differences in Skin: A Review of the Literature. *Gen. Med.* **2007**, *4*, 308–328. [[CrossRef](#)]
33. Xiao, X.; Fang, Y.; Xiao, X.; Xu, J.; Chen, J. Machine-Learning-Aided Self-Powered Assistive Physical Therapy Devices. *ACS Nano* **2021**, *15*, 18633–18646. [[CrossRef](#)] [[PubMed](#)]
34. Luo, Y.; Xiao, X.; Chen, J.; Li, Q.; Fu, H. Machine-Learning-Assisted Recognition on Bioinspired Soft Sensor Arrays. *ACS Nano* **2022**, *16*, 6734–6743. [[CrossRef](#)]
35. Chen, G.; Fang, Y.; Zhao, X.; Tat, T.; Chen, J. Textiles for Learning Tactile Interactions. *Nat. Electron.* **2021**, *4*, 175–176. [[CrossRef](#)]
36. Fang, Y.; Xu, J.; Xiao, X.; Zou, Y.; Zhao, X.; Zhou, Y.; Chen, J. A Deep-Learning-Assisted On-Mask Sensor Network for Adaptive Respiratory Monitoring. *Adv. Mater.* **2022**, *34*, 2200252. [[CrossRef](#)]

37. Guo, R.; Fang, Y.; Wang, Z.; Libanori, A.; Xiao, X.; Wan, D.; Cui, X.; Sang, S.; Zhang, W.; Zhang, H.; et al. Deep Learning Assisted Body Area Triboelectric Hydrogel Sensor Network for Infant Care. *Adv. Funct. Mater.* **2022**, *32*, 2204803. [[CrossRef](#)]
38. Lin, Z.; Zhang, G.; Xiao, X.; Au, C.; Zhou, Y.; Sun, C.; Zhou, Z.; Yan, R.; Fan, E.; Si, S.; et al. A Personalized Acoustic Interface for Wearable Human–Machine Interaction. *Adv. Funct. Mater.* **2022**, *32*, 2109430. [[CrossRef](#)]
39. Meredith, D.J.; Clifton, D.; Charlton, P.; Brooks, J.; Pugh, C.W.; Tarassenko, L. Photoplethysmographic Derivation of Respiratory Rate: A Review of Relevant Physiology. *J. Med. Eng. Technol.* **2011**, *36*, 1–7. [[CrossRef](#)] [[PubMed](#)]
40. Dehkordi, P.; Garde, A.; Molavi, B.; Ansermino, J.M.; Dumont, G.A. Extracting Instantaneous Respiratory Rate from Multiple Photoplethysmogram Respiratory-Induced Variations. *Front. Physiol.* **2018**, *9*, 948. [[CrossRef](#)]
41. Addison, P.S.; Watson, J.N.; Mestek, M.L.; Mecca, R.S. Developing an Algorithm for Pulse Oximetry Derived Respiratory Rate (RRoxi): A Healthy Volunteer Study. *J. Clin. Monit. Comp.* **2012**, *26*, 45–51. [[CrossRef](#)]
42. Shelley, K.H.; Dickstein, M.; Shulman, S.M. The Detection of Peripheral Venous Pulsation Using the Pulse Oximeter as a Plethysmograph. *J. Clin. Monit.* **1993**, *9*, 283–287. [[CrossRef](#)]
43. Alian, A.A.; Shelley, K.H. Photoplethysmography. *Best Pract. Res. Clin. Anaesthesiol.* **2014**, *28*, 395–406. [[CrossRef](#)] [[PubMed](#)]
44. Allen, J. Photoplethysmography and Its Application in Clinical Physiological Measurement. *Physiol. Meas.* **2007**, *28*, R1–R39. [[CrossRef](#)] [[PubMed](#)]
45. Carter, S.A.; Tate, R.B. Value of Toe Pulse Waves in Addition to Systolic Pressures in the Assessment of the Severity of Peripheral Arterial Disease and Critical Limb Ischemia. *J. Vasc. Surg.* **1996**, *24*, 258–265. [[CrossRef](#)]
46. Maeda, Y.; Sekine, M.; Tamura, T. Relationship Between Measurement Site and Motion Artifacts in Wearable Reflected Photoplethysmography. *J. Med. Syst.* **2011**, *35*, 969–976. [[CrossRef](#)]
47. Wong, A.; Pun, K.-P.; Zhang, Y.-T.; Hung, K. A Near-Infrared Heart Rate Measurement IC with Very Low Cutoff Frequency Using Current Steering Technique. *IEEE Trans. Circuits Syst. Regul. Pap.* **2005**, *52*, 2642–2647. [[CrossRef](#)]
48. Chen, G.; Li, Y.; Bick, M.; Chen, J. Smart Textiles for Electricity Generation. *Chem. Rev.* **2020**, *120*, 3668–3720. [[CrossRef](#)]
49. Zhao, X.; Nashalian, A.; Ock, I.W.; Popoli, S.; Xu, J.; Yin, J.; Tat, T.; Libanori, A.; Chen, G.; Zhou, Y.; et al. A Soft Magnetoelastic Generator for Wind Energy Harvesting. *Adv. Mater.* **2022**, 2204238. [[CrossRef](#)]
50. Zhou, Y.; Xiao, X.; Chen, G.; Zhao, X.; Chen, J. Self-Powered Sensing Technologies for Human Metaverse Interfacing. *Joule* **2022**, *6*, 1381–1389. [[CrossRef](#)]
51. Zhou, Y.; Zhao, X.; Xu, J.; Fang, Y.; Chen, G.; Song, Y.; Li, S.; Chen, J. Giant Magnetoelastic Effect in Soft Systems for Bioelectronics. *Nat. Mater.* **2021**, *20*, 1670–1676. [[CrossRef](#)]
52. Chen, G.; Zhao, X.; Andalib, S.; Xu, J.; Zhou, Y.; Tat, T.; Lin, K.; Chen, J. Discovering Giant Magnetoelasticity in Soft Matter for Electronic Textiles. *Matter* **2021**, *4*, 3725–3740. [[CrossRef](#)] [[PubMed](#)]
53. Xiao, X.; Xiao, X.; Zhou, Y.; Zhao, X.; Chen, G.; Liu, Z.; Wang, Z.; Lu, C.; Hu, M.; Nashalian, A.; et al. An Ultrathin Rechargeable Solid-State Zinc Ion Fiber Battery for Electronic Textiles. *Sci. Adv.* **2021**, *7*, eabl3742. [[CrossRef](#)] [[PubMed](#)]
54. Deng, W.; Zhou, Y.; Libanori, A.; Chen, G.; Yang, W.; Chen, J. Piezoelectric Nanogenerators for Personalized Healthcare. *Chem. Soc. Rev.* **2022**, *51*, 3380–3435. [[CrossRef](#)] [[PubMed](#)]